

Functional analysis of organophosphorus hydrolase variants with high degradation activity towards organophosphate pesticides

Catherine Mee-Hie Cho^{1,2}, Ashok Mulchandani¹ and Wilfred Chen^{1,3}

¹Department of Chemical and Environmental Engineering and ²Department of Biochemistry, University of California, Riverside, CA 92521, USA

³To whom correspondence should be addressed.
E-mail: wilfred@engr.ucr.edu

Organophosphorus hydrolase (OPH, also known as phosphotriesterase) is a bacterial enzyme that is capable of degrading a wide range of neurotoxic organophosphate nerve agents. Directed evolution has been used to generate one variant (22A11) with up to 25-fold improved hydrolysis of methyl parathion. Surprisingly, this variant also degraded all other substrates (paraoxon, parathion and coumaphos) tested 2- to 10-fold faster. Since only one mutation (H257Y) is directly located in the active site, site-directed mutagenesis and saturation mutagenesis were used to identify the role of the other distal substitutions (A14T, A80V, K185R, H257Y, I274N) on substrate specificity and activity. Sequential site-directed mutagenesis indicated that K185R and I274N are the most important substitutions, leading to an improvement not only in the hydrolysis of methyl parathion but also the overall hydrolysis rate of all other substrates tested. Using structural modeling, these two mutations were shown to favor the formation of hydrogen bonds with nearby residues, resulting in structural changes that could alter the overall substrate hydrolysis.

Keywords: degradation/directed evolution/methyl parathion/organophosphate pesticides/organophosphorus hydrolase/site-directed mutagenesis

Introduction

Major achievements in agriculture crop production have been obtained by using pesticides for successful pest control. One of the most popular types of pesticide is the organophosphate (OP) family, which effectively eliminates pests owing to its acute neurotoxicity. The effectiveness of OP compounds as pesticides and insecticides also makes them hazardous to humans and to the environment. OPs and their family of compounds are potent neurotoxins that share structural similarities to chemical warfare agents such as sarin, soman and VX [*O*-ethyl-*S*-(2-diisopropylaminoethyl) methylphosphonothioate]. They act as cholinesterase inhibitors and in turn disrupt neurotransmission in both insects and humans.

Among several enzymes that are capable of hydrolyzing OP compounds, organophosphate hydrolase (OPH) has been the most extensively studied because of its ability to hydrolyze a variety of OP neurotoxins including common insecticides and structurally similar chemical warfare agents such as sarin and soman (Dumas *et al.*, 1989). However, hydrolysis rates vary from very fast for paraoxon and parathion to limited hydrolysis

for methyl parathion and chlorpyrifos (Kolakowski *et al.*, 1997; Dumas *et al.*, 1990; Lai *et al.*, 1994). Recently, a similar enzyme (OPDA) with 90% sequence identity to OPH has been isolated from *Agrobacterium radiobacter* (Horne *et al.*, 2002). Subtle changes in substrate specificity have been reported for OPDA, which exhibits higher k_{cat} values for substrates with shorter side chains such as methyl parathion, suggesting that activity and substrate specificity could be altered with relatively few changes in amino acid residues.

Directed evolution is a powerful strategy to create enzyme variants with desirable traits by combining random mutagenesis with focused selection. Both OPH and OPDA have been subjected to directed evolution efforts to improve their catalytic performances and expression levels (Cho *et al.*, 2002, 2004; Griffiths and Tawfik, 2003; Yang *et al.*, 2003; McLoughlin *et al.*, 2005; Roodveldt and Tawfik, 2005). In all cases, mutations far from the active site were found to be involved in the improved properties. However, the functional role of these mutations has not been examined in detail.

Previously, we have generated several OPH variants by DNA shuffling for improved hydrolysis of methyl parathion (Cho *et al.*, 2002). One variant (22A11) in particular exhibits a 25-fold improvement in the methyl parathion hydrolysis rate. Of the five substitutions present in 22A11 (A14T, A80V, K185R, H257Y, I274N), only one (H257Y) is directly located in the active site of OPH, leading to the question of how these distal substitutions contribute to the improved activity and specificity. In this work, the first systematic study was performed to investigate the role of each mutation on the enhanced activity. Site-directed mutagenesis and saturation mutagenesis were carried out to assess the importance of individual and combined effects of these distal mutations in determining substrate specificity and activity on a range of OP pesticides.

Materials and methods

Bacterial strains and plasmids

Escherichia coli strain XL1-Blue {*recA1*, *endA1*, *gyrA96*, *thi-1*, *hsdR17* (r_{k}^- , m_{k}^+), *supE44*, *relA1*, *lac* [*F'*, *proAB*, *lacI^qZAM15*, Tn10 (Tet^r)]} was used in all experiments. The wild-type *opd* gene encoding OPH and its variants genes obtained from previous work were ligated into pP_{ROEX} HTa (GIBCO BRL) to generate pHSOP. This plasmid allowed the intracellular expression of the OPH variants as an N-terminal fusion to a hexahistidine tag (His₆). For site-directed mutagenesis and saturate mutagenesis studies, wild-type *opd* gene and mutants were expressed on the cell surface of *E. coli* using pINCOP containing truncated ice nucleation protein (INPNC) anchor as described in a previous study (Shimazu *et al.*, 2001).

Purification of OPH variants

To determine the kinetic properties of the OPH variants, the OPH wild-type and the variants were expressed as histidine tag fusion and purified using an Ni affinity column. Plasmid-bearing bacterial cultures were grown in 200 ml of Terrific broth supplemented with ampicillin to a final concentration of 100 µg/ml and 10 µM of CoCl₂ at 30°C. Cultures were induced with 1.0 mM IPTG at an OD₆₀₀ of 1.0 and the CoCl₂ concentration was adjusted to 0.1 mM after 4 h of induction. Cell pellets were resuspended in 30 ml of binding buffer (50 mM sodium phosphate pH 8.0, 300 mM NaCl and 1% Triton X-100) with 0.1 mM CoCl₂ added. Benzonase (Novagen) and protease inhibitor, AEBSF (Calbiochem), were added at 37°C for 20 min. Cells were cooled to 0°C and passed through a French pressure cell (15 000–20 000 psi). The solution was centrifuged for 10 min at 20 000 g. The resulting solution was added to a His-Bind Quick column (Novagen), which was pre-washed with 15 ml of the binding buffer. The column was washed with 30 ml of binding buffer, followed by 25 ml of washing buffer (50 mM phosphate pH 8.0, 500 mM NaCl, 10% glycerol and 25 mM imidazole). Enzymes were eluted with 10 ml of elution buffer (50 mM sodium phosphate pH 8.0, 300 mM NaCl, 5% glycerol) containing 200 mM imidazole and each 1 ml fraction was collected using a fraction collector (BioRad, Hercules, CA). All eluted fractions were tested for OPH activity and protein purity by SDS-PAGE. Fractions with the highest OPH activity were pooled and then the elution buffer was changed to 50 mM CHES buffer pH 9.0 containing 0.05 mM CoCl₂ using PD010 columns (Amersham Bioscience, Uppsala, Sweden) to remove imidazole.

Organophosphorus hydrolase assay

The kinetic constants for each variant were obtained by measuring the initial hydrolysis rate of the substrate at different concentrations using a constant enzyme concentration. The enzyme was diluted with citrate-phosphate buffer pH 8.0 containing 0.1 mM CoCl₂ in the presence of 1 mg/ml bovine serum albumin (BSA), which was used to stabilize the diluted protein. The change in absorbance (412 nm, ε₄₁₂ = 16 500 M⁻¹ cm⁻¹ for *p*-nitrophenol) was measured in 50 mM phosphate-citrate buffer pH 8.0 containing either methyl parathion or paraoxon, 10% methanol and 0.1 mM CoCl₂ in 1.5 ml disposable methacrylate cuvettes (Fisher) with a Beckman DU-60 spectrophotometer for 5 min at 37°C. All assays were performed in triplicate. Enzyme concentrations were determined according to the Bradford method (BioRad) using BSA as the standard. The kinetic constants (*K_m* and *k_{cat}*) were obtained by fitting the data to Lineweaver-Burk reciprocal plot (Equation 1) and Hanes-Woolf plot (Equation 2):

$$\frac{1}{v} = \frac{K_m}{V_{max}} \times \frac{1}{[S]} + \frac{1}{V_{max}} \quad (1)$$

$$\frac{[S]}{v} = \frac{1}{V_{max}} \times [S] + \frac{K_m}{V_{max}} \quad (2)$$

where *v* = velocity, *V_{max}* = maximum velocity, [S] = substrate concentration and *K_m* is the Michaelis constant. *k_{cat}* is calculated according to the equation *k_{cat}* = *V_{max}*/*E*, where *E* is the protein concentration used in the assay.

For the whole cell assays, cells were grown at 30°C in Lurie-Bertani (LB) medium containing 100 µg/ml ampicillin. After 25 h of growth, 0.1 mM CoCl₂ was added and cells were harvested after 48 h. For each assay, 100 µl of a cell suspension expressing different variants on the cell surface (OD₆₀₀ = 2.0) was resuspended in 0.9 ml of 50 mM phosphate-citrate buffer (pH 8.0) containing 0.1 mM CoCl₂ and 0.1 ml of substrate in methanol was added to measure the hydrolysis rate at 37°C for 2 min. The concentrations used in the assay for paraoxon, methyl parathion, parathion and coumaphos were 2, 0.5, 0.5 and 0.2 mM, respectively. The rate of methyl parathion, paraoxon and parathion hydrolysis was measured by monitoring the appearance of *p*-nitrophenol at 412 nm (ε₄₁₂ = 16 500 M⁻¹ cm⁻¹) as described above. The rate of coumaphos hydrolysis was measured by measuring the production of chlorferon at 348 nm (ε₃₄₈ = 9100 M⁻¹ cm⁻¹ at pH 8.0). The expression level of different variants was probed by western blot analysis using INPNC antisera (Cho *et al.*, 2002).

Site-directed mutagenesis

The mutation K185R was incorporated in OPH wild-type using a QuikChange Mutagenesis Kit (Stratagene). The template was INCOP. The primers were 185RF, 5'-C TTT CAG GAG TTA GTG TTA AGG GCG GCC-3' and 185RR, 5'-GGC CGC CCT TAA CAC TAA CTC CTG AAA G-3'. Mutation K185E was introduced in 22A11. The primers were 185EF, 5'-C TTT CAG GAG TTA GTG TTA GAG GCG GCC-3' and 185ER, 5'-GGC CGC CTC TAA CAC TAA CTC CTG AAA G-3'. The mutants obtained from site-directed mutagenesis were sequenced to confirm the presence of each mutation. A combination of A80V/I274N/K185R (2H2 + 5A6R) was constructed by cloning a gene using 2H2 (A80V) and 5A6R (I274N/K185R) gene. The plasmid containing 2H2 variants, pINCOP-2H2, served as a vector. The plasmid containing 5A6R obtained from site-directed mutagenesis was digested with *SalI* and *HindIII* to liberate 933 bp fragments containing I274N/K185R mutations. Then the fragments were ligated into *HindIII/SalI*-digested pINCOP-2H2 to generate A80V/I274N/K185R mutant.

Saturation mutagenesis

Site-specific saturation mutagenesis at Arg185-Asn274 on INCOP-22A11 variant was performed using a QuikChange Multi Site-Directed Mutagenesis kit (Stratagene) according to the manufacturer's instructions. The degenerated oligonucleotides sequences used as primers were 185DeR, 5'-GGG CGG CCG CHN NTA ACA CTA ACT CCT GAA AG-3' and 274DeR, 5'-GTG TTT GCC ACG AAC GHN NGC CCA GGA G-3'. The degenerated sequence was incorporated into 22A11 gene by PCR amplification with a program of 1 min at 95°C, 30 cycles of 1 min at 95°C, 1 min at 60°C and 10 min at 67°C, followed by 10 min at 67°C. Restriction enzyme *DpnI* was added to digest parent templates and then fragments were transformed into *E.coli*. Library of cells were screened for methyl parathion hydrolysis activity in comparison with the activity of 22A11 using a 'Top Agar' plate assay and microplate assay as described in a previous study (Cho *et al.*, 2002). Randomly selected variants were sequenced to ensure the presence of diverse amino acid substitution.

Structural models

The model structure of the OPH variant 22A11 was obtained in comparison with the wild-type OPH structure (1eyw.pdb)

Table I. Kinetic parameters of purified OPH variants for methyl parathion and paraoxon^{a,b}

Compound	Protein	K_m (mM)	k_{cat} (s ⁻¹)	k_{cat}/K_m (s ⁻¹ M ⁻¹)	
Methyl parathion	Wild-type	1.22 ± 0.03	2300 ± 130	1.9 × 10 ⁶	
	2H2	1.89 ± 0.08	11400 ± 950	6.0 × 10 ⁶	
	5A6	2.01 ± 0.05	24000 ± 1540	1.2 × 10 ⁷	
	6D4	0.58 ± 0.03	18300 ± 1030	3.2 × 10 ⁷	
	21E1	0.74 ± 0.02	25100 ± 2950	3.4 × 10 ⁷	
	22D8	0.61 ± 0.02	19100 ± 740	3.1 × 10 ⁷	
	22A11	0.62 ± 0.02	39600 ± 2100	6.4 × 10 ⁷	
	2H2R	1.62 ± 0.03	13300 ± 1030	8.2 × 10 ⁶	
	5A6R	0.99 ± 0.02	20000 ± 1330	2.0 × 10 ⁷	
	2H2 + 5A6R	0.88 ± 0.06	16000 ± 800	1.8 × 10 ⁷	
	Paraoxon	Wild-type	0.12 ± 0.003	11700 ± 580	1.0 × 10 ⁸
		2H2	0.16 ± 0.02	65500 ± 2430	4.1 × 10 ⁸
5A6		0.13 ± 0.01	74400 ± 4460	5.7 × 10 ⁸	
6D4		0.23 ± 0.01	32700 ± 1630	1.4 × 10 ⁸	
22A11		0.16 ± 0.01	101300 ± 1540	6.2 × 10 ⁸	
2H2R		0.21 ± 0.02	157600 ± 3080	7.5 × 10 ⁸	
5A6R		0.064 ± 0.004	81400 ± 4940	1.3 × 10 ⁹	
2H2 + 5A6R		0.16 ± 0.02	176500 ± 7510	1.1 × 10 ⁹	

^aFirst round: 2H2: A80V, S365P; 2F6: L182S, V310A; 5A6: I274N; 6D4: H257Y. Second round: 21E1: H257Y, I274N, S365P; 22D8: L130M, H257Y, I274N; 22A11: A14T, A80V, K185R, H257Y, I274N. Site-directed mutagenesis: 2H2R: A80V, K185R; 5A6R: I274N, K185R. 2H2 + 5A6R: A80V, K185R, I274N.

^bAll variants were purified as a His-tagged enzyme.

using Swiss-Model, which was provided by the ExpASY molecular biology server of the Swiss Institute of Bioinformatics (Guex and Peitsch, 1997; Schwede *et al.*, 2003). The structural analysis of mutations was carried out using PDBViewer (v3.7). Force field energy, steric hindrance favorable interactions and energy minimization were employed to predict the side-chain structure of each mutation.

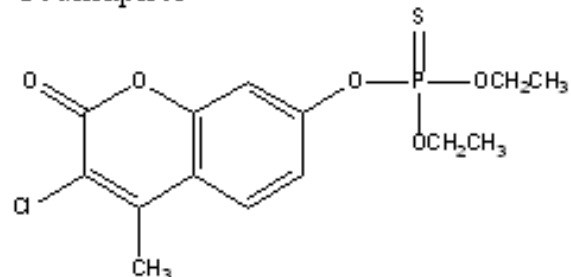
Results

Characterization of improved variants for methyl parathion degradation

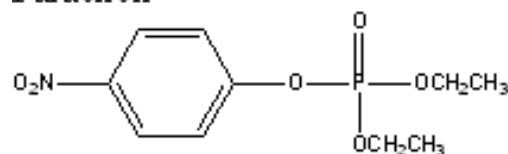
In a previous study, several OPH variants with enhanced hydrolysis of methyl parathion were obtained using DNA shuffling (Cho *et al.*, 2002). Most of mutations identified were not directly located in the active site and their functions are not clearly understood. To characterize the evolved variants for improved methyl parathion degradation, the catalytic constants k_{cat} and K_m for selected variants were measured and the results are summarized in Table I. Most first round variants had significantly increased k_{cat} values, while K_m values were slightly increased. Only one variant, 6D4, containing the H257Y mutation, appears to improve substrate binding resulting in a 2-fold reduction in K_m . This is consistent with previous reports indicating the importance of this substitution in reducing the size of the larger binding pocket and favors binding of substrates with smaller substituents (Di Sioudi *et al.*, 1999; Wu *et al.*, 2000). This is also supported by the presence of a tyrosine residue at position 257 in OPDA, which results in enhanced activity towards methyl parathion (Horne *et al.*, 2002). The substitution of I274N had the most significant impact on increasing k_{cat} . This mutation is located on a mobile loop supporting the large binding pocket (Koca *et al.*, 2001; Yang *et al.*, 2003) and this solvent-exposed residue has been suggested to affect enzyme activity through the dynamics of the surface loop (Yang *et al.*, 2003).

Diethyl

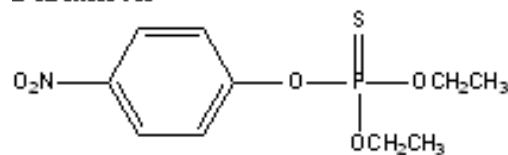
Coumaphos



Paraoxon



Parathion



Dimethyl

Methyl parathion

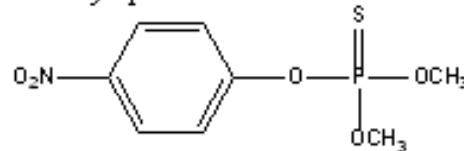


Fig. 1. Chemical structure of substrates used in this study. Substrates are grouped based on their dimethyl or diethyl side chains.

All second-round variants tested contained the H257Y/I274N double mutations identified from the first round. However, except for 22A11, the k_{cat} and K_m values of 22D8 and 21E1 were similar to those of 6D4. The additional substitution of L130M in 22D8 also appears to be neutral since virtually no change in k_{cat}/K_m was observed on comparing with 21E1. In contrast, the presence of additional K185R and A80V mutations in the best variant (22A11) increased the overall catalytic efficiency by another 2-fold. In this case, K_m remained similar to other second-round variants, whereas k_{cat} almost doubled in value. Interestingly, these two mutations have also been identified in other recent directed evolution studies with OPH or OPDA (Yang *et al.*, 2003; McLoughlin *et al.*, 2005;

Roodveldt and Tawfik, 2005). The presence of either A80V or K185R was associated with an increase in enzyme stability and expression level rather than an increase in activity. However, our results clearly indicate that the A80V and K185R mutations

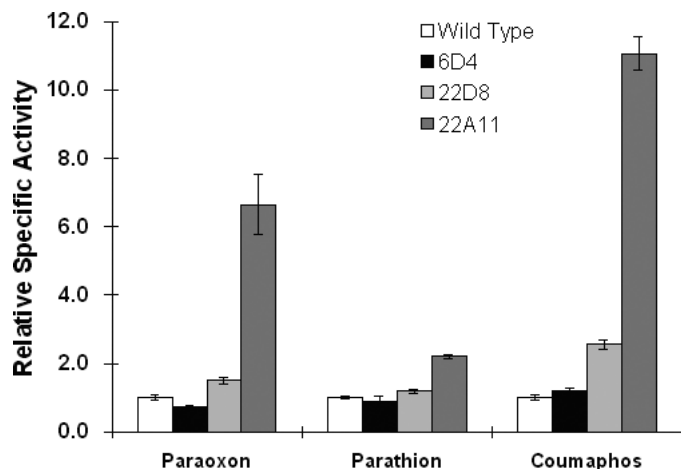


Fig. 2. Hydrolysis of paraoxon, parathion and coumaphos by whole cell expressing OPH variants on the cell surface. Results are expressed as whole cell activities normalized to that of cells expressing the wild-type OPH.

are responsible for the 2-fold improvement in k_{cat}/K_m for 22A11.

The importance of the additional K185R and A80V mutations in 22A11 was further investigated by comparing the degradation rates of other substrates containing the larger diethyl side chain such as paraoxon, parathion and coumaphos (Figure 1) with whole cells expressing the different variants on the cell surface. We have previously demonstrated that the specific activities of purified OPH variants were well correlated with the whole-cell activity assays (Cho *et al.*, 2002). More importantly, no difference in OPH expression was detected in all cases, validating the use of surface display of OPH as a rapid method of comparing the activity towards different substrates without any limitation on substrate accessibility.

From the whole cell assay, only 22A11 was shown to hydrolyze all these substrates substantially better than the wild-type OPH (from 2- to 10-fold), little improvement being observed with other variants (Figure 2). This was unexpected because these variants were selected to favor the hydrolysis of methyl parathion, a substrate containing the smaller dimethyl side chain. These results suggest that the additional K185R/A80V mutations in 22A11 are responsible for not only or increasing methyl parathion hydrolysis but perhaps also the overall hydrolysis rate of OPH. Since the paraoxon hydrolysis

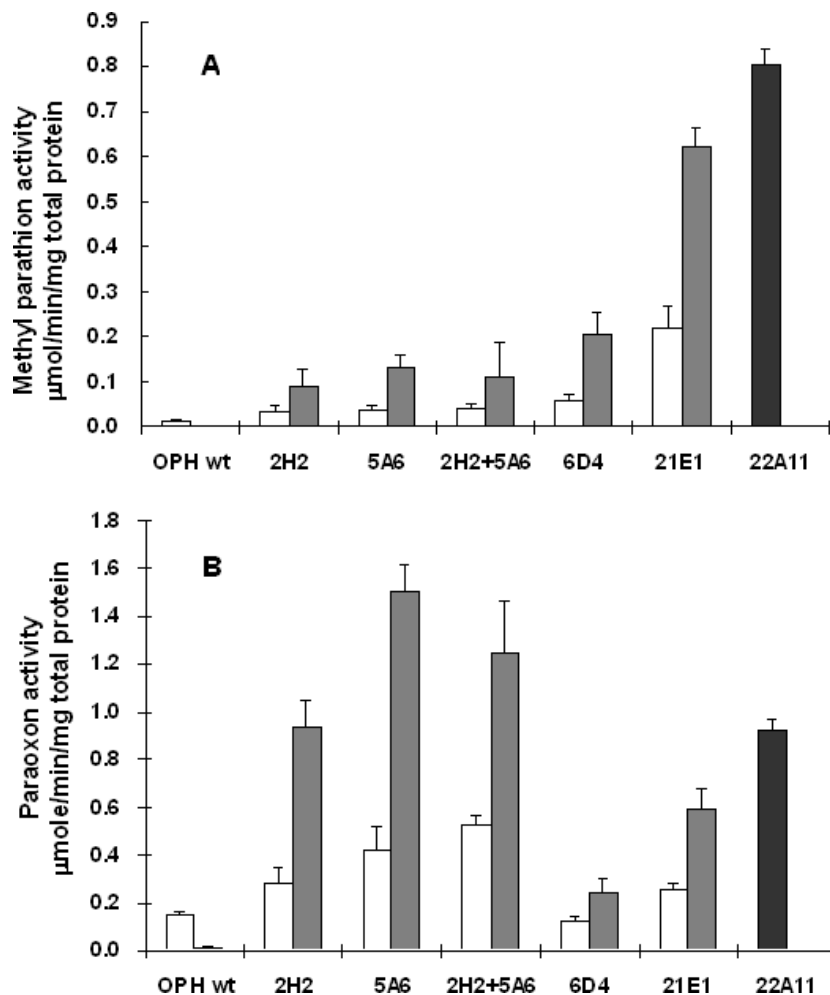


Fig. 3. Hydrolysis of (A) methyl parathion and (B) paraoxon by whole cells expressing OPH variants generated by site-directed mutagenesis. The K185R mutation (gray bar) was added to first- and second-round variants (white bar) selected for improved methyl parathion hydrolysis. Variant 2H2 + 5A6 contained the double A80V/I274N mutations. A detailed description of all the variants is provided in Table I.

rate by wild-type OPH is already close to the diffusion-control limit, it is striking that 22A11 could hydrolyze this substrate 6-fold faster. However, this improvement was further confirmed by comparing the kinetic constants with the k_{cat} value of 22A11 almost 9-fold higher than the wild-type (Table I).

Functional analysis by site-directed mutagenesis

To investigate the functional roles of A80V, K185R and I274N on substrate specificity and activity, we resorted to site-directed mutagenesis to determine how each mutation or combined mutations affect the catalytic efficiency and to postulate a relationship between the mutations and functionality of the variants. Initially, the effect of the K185R mutation was tested. Surprisingly, whole-cell activity was lost almost completely for both methyl parathion and paraoxon when this mutation was incorporated into the wild-type OPH (Figure 3). Apparently, this mutation by itself is detrimental to functionality, suggesting that it may alter the global structure of the enzyme by the potential hydrogen bonding to Glu219 or Glu181 as suggested (Yang *et al.*, 2003). To investigate whether there is a synergistic effect between the K185R mutation and the other mutations, the K185R mutation was introduced into three first-round variants containing a single mutation (2H2:A80V, 5A6:I274N and 6D4:H257Y), a new variant 2H2 + 5A6 containing a combination of two single mutations (A80V and I274N) and the second-round variant, 21E1, containing only H257Y/I274N. The introduction of K185R increased the whole-cell hydrolytic activity against methyl parathion significantly for all combinations tested (Figure 3A). These results indicate that K185R must be present in conjunction with other mutations to be beneficial. When the K185R substitution was added into 21E1, methyl parathion hydrolysis was improved by more than 2-fold to a level similar to that of 22A11, suggesting that the K185R substitution may be more important than A80V in improving the overall hydrolytic rate. The catalytic constants, K_m and k_{cat} , for selected mutants with the additional K185R substitution were also examined (Table I). When K185R was introduced into A80V (2H2R), a minor reduction in K_m and a slight increase in k_{cat} were observed, resulting in a 35% increase in the catalytic efficiency. Combining K185R with I274N (5A6R) increased k_{cat}/K_m by 80%, whereas the addition of A80V into 5A6R (2H2 + 5A6R) did not substantially alter the values of K_m and k_{cat} , again indicating that the K185R and I274N mutations are more important in improving the overall catalytic activity.

The effect of the K185R mutation on improving the overall hydrolysis rate was similarly observed for paraoxon (Figure 3B). Surprisingly, even variants carrying the A80V (2H2) or I274N (5A6) single mutation improved the paraoxon hydrolysis rate by more than 2-fold, suggesting that these mutations may also affect the overall catalytic efficiency. Similar results were also obtained with purified enzymes (Table I), where the presence of A80V or I274N alone increased the k_{cat} values by 4- to 5-fold with virtually no change in K_m .

The 5A6R mutant (I274N/K185R) without the H257Y mutation exhibited the highest paraoxon hydrolysis rate. This result is expected because the H257Y mutation favors substrates with a smaller dimethyl side chain. The addition of K185R into I274N (5A6R) represented a 2-fold reduction in K_m with a slightly increased k_{cat} . In contrast, when A80V was combined with I274N (2H2 + 5A6), only a minor additive effect on paraoxon degradation was observed. Addition of the A80V

Table II. Hydrolysis of methyl parathion and paraoxon by whole cells carrying mutants generated by saturation mutagenesis

	Amino acid substitution		Specific activity (mmol/min.mg total protein)	
			Methyl parathion	Paraoxon
OPH wt	K185	I274	0.013	0.143
22A11	R185 (AGG)	N274 (AAC)	0.796	0.918
STD2024	R185R (AGG)	N274K (AAA)	0.787	1.37
STD1	R185T (ACG)	N274N (AAT)	N/A	N/A
STD2	R185F (TTT)	Z (TAA)	N/A	N/A
STD3	Z (TGA)	N274W (TGG)	N/A	N/A
STD4	R285Q (CAG)	N274Q (CAG)	N/A	N/A
STD5	R185P (CCT)	N274R (AGA)	N/A	0.011
STD6	R185N (AAT)	N274I (ATT)	N/A	0.004
STD7	R185N (AAT)	N274G (GGT)	0.0003	0.037
STD8	R185S (AGT)	N274L (TTG)	0.006	0.057
STD9	R185S (TCT)	N274N (AAC)	0.011	0.033
STD10	R185G (GGA)	N274E (GAA)	0.011	0.033
STD11	R185P (CCA)	N274Y (TAT)	0.016	0.038
STD12	R185C (TCT)	N274V (GTG)	0.017	0.09
STD13	R185N (AAT)	N274S (TCT)	0.024	0.034
STD14	R185I (ATT)	N274E (GAG)	0.061	0.066
STD15	R185V (GTT)	N274K (AAA)	0.065	0.062
STD16	R185Q (CAA)	N274G (GGA)	0.096	0.099
STD17	R185Q (CAG)	N274V (GTT)	0.135	0.332
STD18	R185Q (CAA)	N274N (AAT)	0.162	0.156
STD19	R185Q (CAA)	N274K (AAG)	0.164	0.195
STD20	R185H (CAT)	N274I (ATA)	0.314	0.564
STD21	R185R (AGG)	N274S (TCT)	0.469	0.694

mutation into 5A6R reduced the k_{cat}/K_m for paraoxon hydrolysis by 20%, again indicating that the K185R and I274 substitutions are more important than A80V in enhancing the overall hydrolysis rate in 22A11.

Enzyme evolution by saturation mutagenesis

To investigate whether other amino acid substitutions at the 185 and 274 positions could further improve the hydrolytic efficiency, saturation mutagenesis was used to incorporate all 20 possible amino acids at these locations. A total of 2436 clones from the library produced by saturation mutagenesis were screened for improved methyl parathion degradation using the 'Top Agar' plate assay described previously (Cho *et al.*, 2002). A large fraction of the library lost activity, indicating that only limited amino acid residues could be substituted at these two locations. Out of 2436 clones screened, 45 potential variants were selected with similar activities when compared with the best variant, 22A11, and these were subjected to further analysis using the microplate assay (the intensity of yellow color formation of *p*-nitrophenolate was compared with the wild-type and 22A11). Only one clone, STD2024, exhibited enhanced activity towards paraoxon and the same level of activity for methyl parathion. In order to verify the efficiency of saturation mutagenesis, 21 clones were chosen for sequencing and the results revealed that the two positions were altered in an unbiased fashion with each nucleotide position being fully randomized (Table II). The ability of all these clones to hydrolysis methyl parathion and paraoxon hydrolysis activity was further tested to study the structural basis for the loss of activity or activity enhancement. The results indicate that positively charged amino acid groups, such as histidine or arginine, are favored at the 185 position in order to retain the enhanced activity. The preference for positively charged amino acids at the 185 position was also

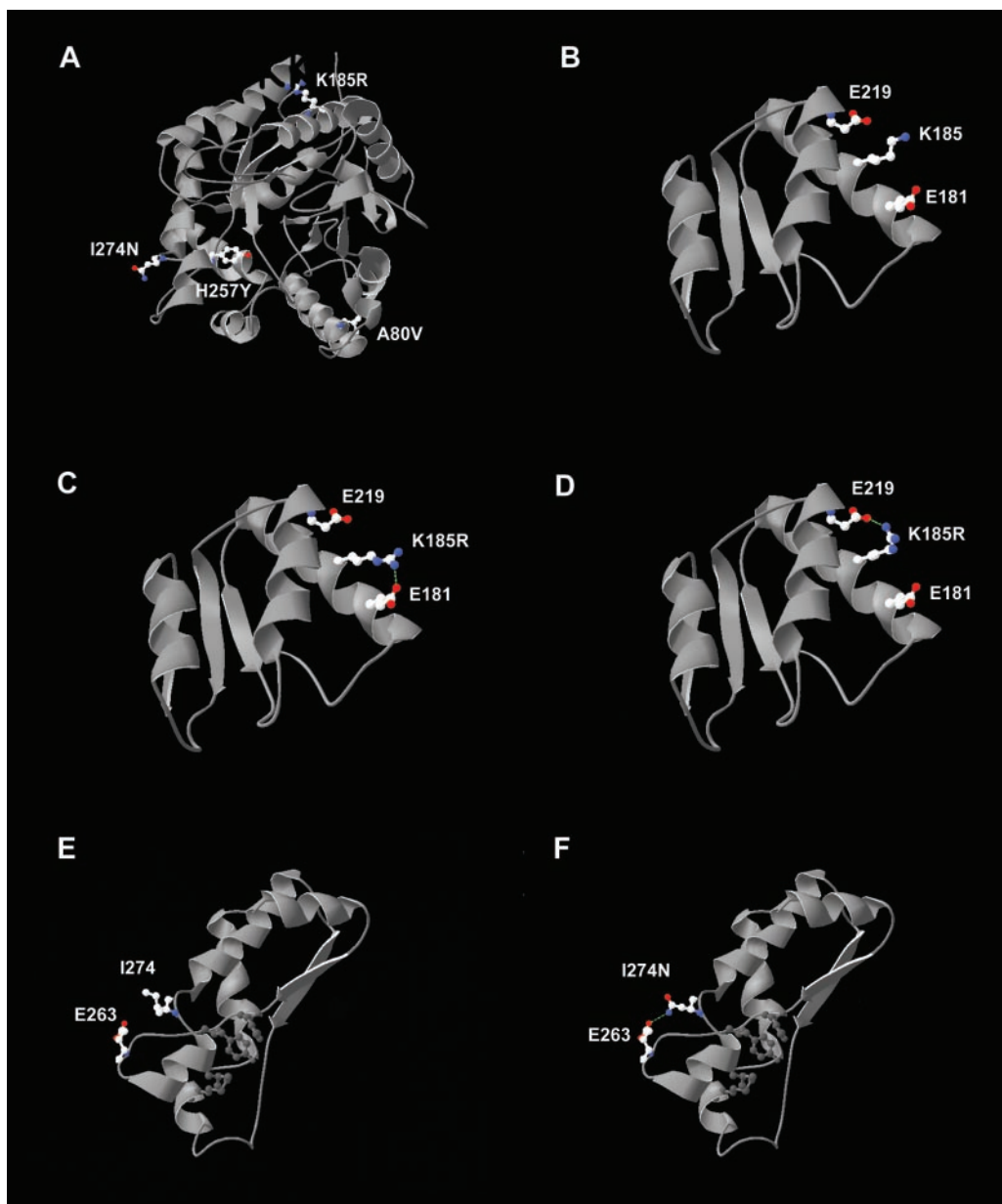


Fig. 4. (A) Ribbon representation of the monomeric structure of OPH. The amino acid residues substituted in 22A11 are highlighted. (B) Location of Lys185 and its neighboring amino acid residues in the wild-type OPH. (C), (D) H-bond formation between K185R and neighboring amino acid residues Glu181 and Glu 219, respectively, using the model structure of 22A11. (E) Partial view of an exposed loop with location of Ile274 that follows strand 7, which supports the large sub-site residues His254 and His257. (F) H-bond formation of I274N using the model structure of 22A11. Amino acids forming the large binding pockets are shown in dark gray.

tested by incorporation of a negatively charged glutamic acid (K185E) residue into both the wild-type OPH and 22A11. This substitution resulted in a total loss of activity (data not shown), supporting the importance of a positively charged residue at this position. On the other hand, position 274 is more flexible as many different charged or uncharged residues can be substituted without any significant loss of activity. The best clone (STD2024) contained an N274K substitution, resulting in a 50% increase in activity for paraoxon compared with 22A11, while maintaining the methyl parathion degradation rate.

Discussion

Since most of the important mutations responsible for improved hydrolysis occurred on or near the enzyme surface,

molecular modeling was used to assess their potential roles in activity enhancement (Figure 4A). One of the mutations, K185R, is located on the outer helix of the external surface, which is more than 20 Å away from active site. It has been suggested that the conversion of K185R allows the formation of hydrogen bonds to Glu219 or Glu181 (Yang *et al.*, 2003). Structural analysis showed that Arg185 could form a hydrogen bond either to Glu181 with a distance of 2.75 Å or to Glu219 at 2.74 Å, whereas Lys185 in the wild-type OPH does not form any hydrogen bond to either E181 or E219 (Figure 4B–D). The same K185R mutation has also been implicated in enhanced OPH expression through increasing the stability of the apoenzyme (Roodveldt and Tawfik, 2005). However, our results suggest that these hydrogen bonds may also enhance the overall hydrolytic activity (mainly through increasing k_{cat}) via

improved OPH stability or conformational change of OPH to favor transition state. In addition, the K185R mutation is located closest to the leaving group site, and it may also interact with the leaving group of the substrates (Vanhook *et al.*, 1996; Benning *et al.*, 2000), resulting in increased hydrolysis.

The second mutation, I274N, resides on the external loop followed by strand 7, supporting the large binding pocket (Figure 4E and F). It has been shown that this loop region (Gly251 to Ser276) is disordered and could change the structure significantly in the absence of metal ions (Benning *et al.*, 1995). Yang *et al.* (2003) also suggested that mutations in this region may affect enzymatic activity through the dynamics of a surface loop. In addition, a molecular dynamics study of the theoretical binding of paraoxon indicated that various conformational changes are involved in substrate positioning in the active site, which coordinates substrate to align with metal ions, resulting in strong polarization of the reaction center of the substrate (Koca *et al.*, 2001). Similar conformational changes have also been reported for OPDA (Jackson *et al.*, 2005). From our structural modeling, the I274N substitution could potentially form a hydrogen bond with the carboxylate oxygen of E263, which has a high *B*-factor, increasing the conformational adaptability of the enzyme to substrate binding.

Acknowledgement

This work was supported by a grant from the USDA (99-35102-8597).

References

- Benning, M.M., Kuo, J.M., Raushel, F.M. and Holden, H.M. (1995) *Biochemistry*, **34**, 7973–7978.
- Benning, M.M., Hong, S.-B., Raushel, F.M. and Holden, H.M. (2000) *J. Biol. Chem.*, **275**, 30556–30560.
- Cho, C.M.-H., Mulchandani, A. and Chen, W. (2002) *Appl. Environ. Microbiol.*, **68**, 2026–2030.
- Cho, C.M.-H., Mulchandani, A. and Chen, W. (2004) *Appl. Environ. Microbiol.*, **70**, 4681–4685.
- Di Sioudi, B.D., Miller, C.E., Lai, K., Grimsley, J.K. and Wild, J.R. (1999) *Chem. Biol. Interact.*, **119–120**, 211–223.
- Dumas, D.P., Caldwell, S.R., Wild, J.R. and Raushel, F.M. (1989) *J. Biol. Chem.*, **261**, 19659–19665.
- Dumas, D.P., Durst, H.D., Landis, W.G., Raushel, F.M. and Wild, J.R. (1990) *Arch. Biochem. Biophys.*, **227**, 155–159.
- Griffiths, A.D. and Tawfik, D.S. (2003) *EMBO J.*, **22**, 24–35.
- Guex, N. and Peitsch, M.C. (1997) *Electrophoresis*, **18**, 2714–2723.
- Horne, I., Sutherland, T.D., Harcourt, R.L., Russell, R.J. and Oakeshott, J.G. (2002) *Appl. Environ. Microbiol.*, **68**, 3371–3376.
- Jackson, C.J., Liu, J.W., Coote, M.L. and Ollis, D.L. (2005) *Organic and Biomol. Chem.*, **3**, 4343–4350.
- Koca, J., Zhan, C.-G., Rittenhouse, R.C. and Ornstein, R.L. (2001) *J. Am. Chem. Soc.*, **123**, 817–826.
- Kolakowski, J.E., DeFrank, J.J., Harvey, S.P., Szafraniec, L.L., Beaudry, W.T., Lai, K.H. and Wild, J.R. (1997) *Biocatalysis and Biotransformation*, **15**, 297–312.
- Lai, K., Dave, K.I. and Wild, J.R. (1994) *J. Biol. Chem.*, **269**, 16579–16584.
- McLoughlin, S.Y., Jackson, C., Liu, J.-W. and Ollis, D. (2005) *Protein Expr. Purif.*, **41**, 433–440.
- Roodveldt, C. and Tawfik, D.S. (2005) *Protein Eng. Des. Sel.*, **18**, 51–58.
- Schwede, T., Kopp, J., Guex, N. and Peitsch, M.C. (2003) *Nucleic Acids Res.*, **31**, 3381–3385.
- Shimazu, M., Mulchandani, A. and Chen, W. (2001) *Biotechnol. Prog.*, **17**, 76–80.
- Vanhook, J.L., Benning, M.N., Raushel, F.M. and Golden, H.M. (1996) *Biochemistry*, **35**, 6020–6025.
- Watkins, L.M., Mahoney, J.J., McCulloch, J.K. and Raushel, F.M. (1997) *J. Biol. Chem.*, **272**, 25596–25601.
- Wu, F., Li, W.-S., Chen-Goodspeed, M., Sogorb, M.A., Raushel, F.M. (2000) *J. Am. Chem. Soc.*, **122**, 10206–10207.

Yang, H., Carr, P.D., McLoughlin, S.Y., Liu, J.W., Horne, I., Qiu, X., Jeffries, C.M.J., Russell, R.J., Oakeshott, J.G. and Ollis, D.L. (2003) *Protein Eng.*, **6**, 135–145.

Received July 8, 2005; revised November 23, 2005; accepted December 1, 2005

Edited by Dan Tawfik